ADVANCED MATERIALS

# Supporting Information

for *Adv. Mater.*, DOI: 10.1002/adma.201604778

## High-Operating-Temperature Direct Ink Writing of Mesoscale Eutectic Architectures

*J. William Boley, Kundan Chaudhary, Thomas J. Ober, Mohammadreza Khorasaninejad, Wei Ting Chen, Erik Hanson, Ashish Kulkarni, Jaewon Oh, Jinwoo Kim, Larry K. Aagesen, Alexander Y. Zhu, Federico Capasso, Katsuyo Thornton, Paul V. Braun, and Jennifer A. Lewis**

Submitted to ADVANCED MATERIALS


**Supporting Information**

# High Operating Temperature Direct Ink Writing Of Mesoscale Eutectic Architectures

J. William Boley, Kundan Chaudhary, Thomas J. Ober, Mohammadreza Khorasaninejad, Wei-Ting Chen, Erik Hanson, Ashish Kulkarni, Jaewon Oh, Jinwoo Kim, Larry K. Aagesen, Alexander Y. Zhu, Federico Capasso, Katsuyo Thornton, Paul V. Braun, and Jennifer A. Lewis*

Dr. J. W. Boley, K. Chaudhary, Dr. T. J. Ober, Prof. J. A. Lewis
John A. Paulson School of Engineering and Applied Sciences
Wyss Institute for Biologically Inspired Engineering
Harvard University
Cambridge MA 02138, USA
Email: jalewis@seas.harvard.edu

Dr. M. Khorasaninejad, Dr. W.T. Chen, A. Y. Zhu, Prof. F. Capasso
John A. Paulson School of Engineering and Applied Sciences
Harvard University
Cambridge, MA 02138, USA

J. Oh
University of Waterloo
Waterloo, ON N2L 3G1, Canada

E. Hanson, Dr. L. K. Aagesen Prof. K. Thornton
Department of Materials Science and Engineering
University of Michigan
Ann Arbor, MI 48109, USA

A. Kulkarni, J. Kim, Prof. P. V. Braun
Department of Materials Science and Engineering
Frederick Seitz Materials Research Laboratory
University of Illinois at Urbana-Champaign
Urbana, IL 61801, USA

Keywords: 3D printing, eutectics, self-assembly, metamaterials, structural color

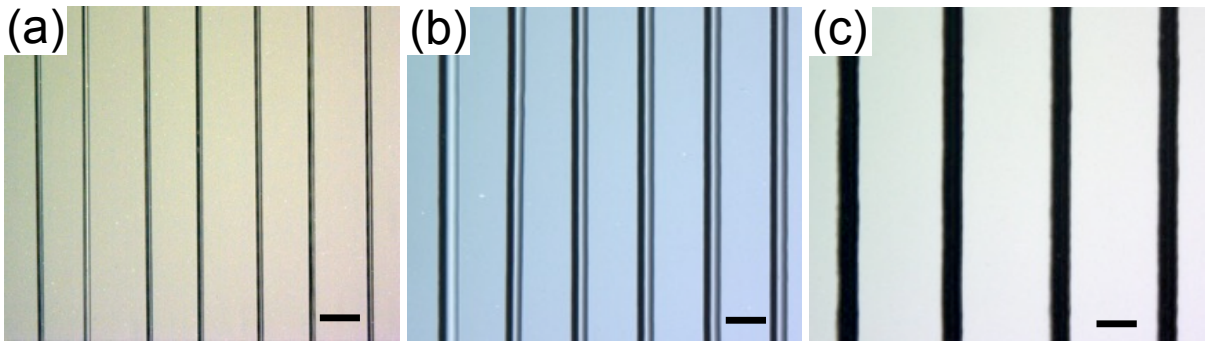


**Figure S1. HOT-DIW printing of molten polymer, carbohydrate glass, and metallic alloy inks.** One-dimensional (1D) arrays of printed filaments (nozzle diameter = 50 μm, nozzle temperature ~ 200°C, substrate temperature ~ 25°C) composed of (a) polylactic acid (PLA). (b) sugar, and (c) eutectic bismuth-tin (Bi-Sn) alloy. Scale bars are 100 μm in length.

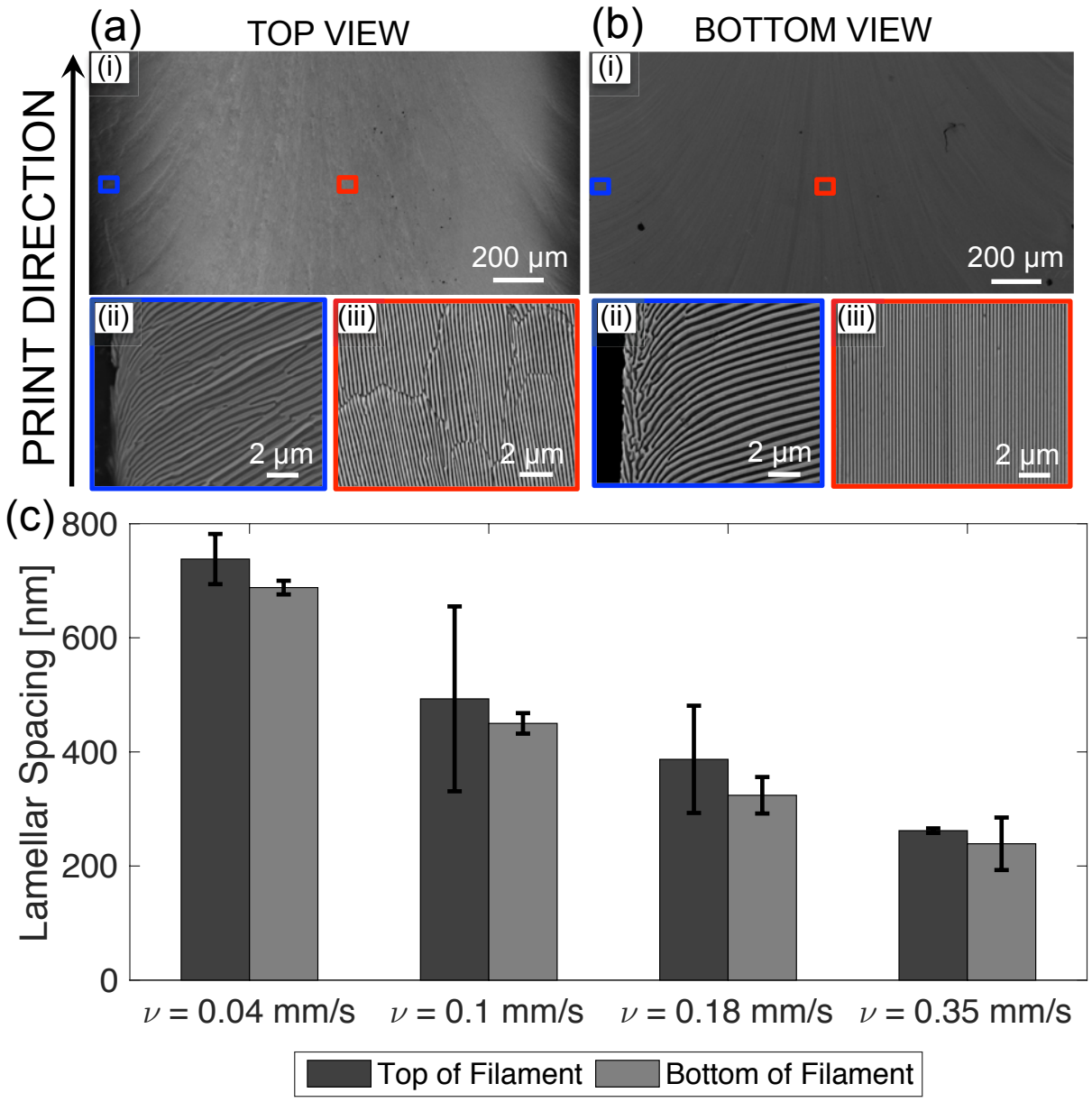


**Figure S2. Lamellar features within printed eutectic AgCl-KCl filaments.** SEM images of the (a) top surface and (b) bottom surface of representative filament (nozzle diameter = 1 mm, nozzle temperature ~ 400°C, substrate temperature ~ 25°C, and $v$ = 0.35 mm·s$^{-1}$), including (i) macro-view and micro-views of (ii) side and (iii) middle of the filament. (c) Bar plot of average lamellar spacing, $L$, as a function of printing speed, $v$, measured at the middle of the filament. Error bars represent ± 2 standard deviations.

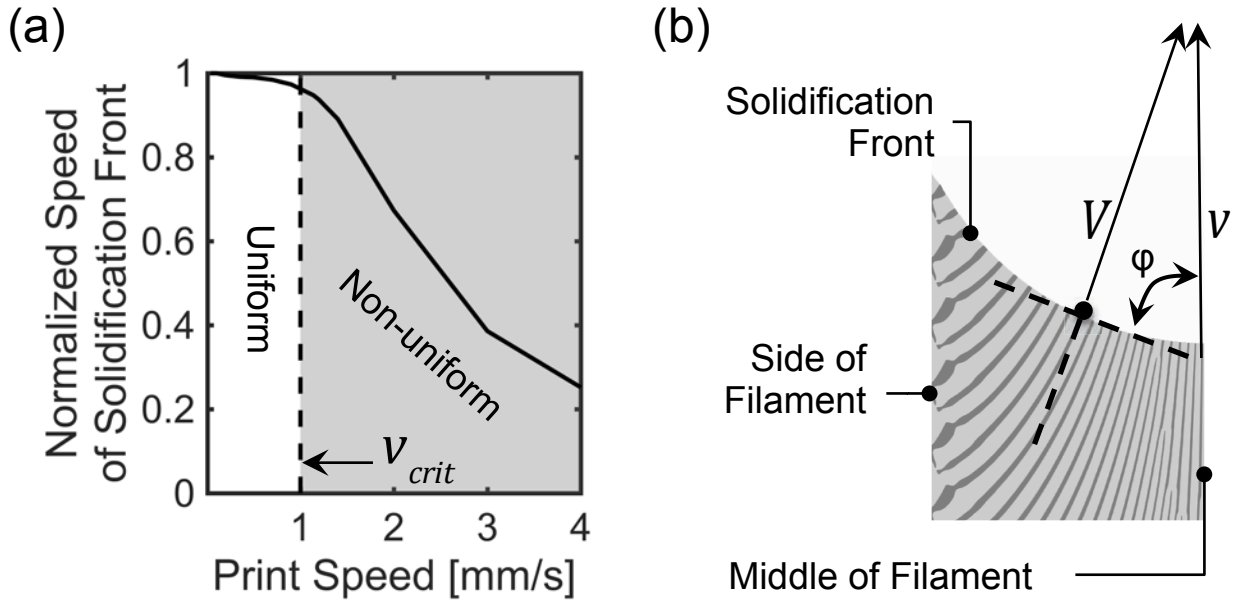


**Figure S3.** (a) Normalized speed of solidification front calculated in the central region of printed filaments as a function of print speed. White region denotes filaments printed below $v_{crit}$, where lamellae of uniform orientation were observed. Gray region denotes filaments printed above $v_{crit}$, exhibiting non-uniformly oriented lamellae. (b) Schematic illustration of lamellar growth along bottom surface of the printed filaments depicting geometric relationship between solidification front velocity ($V$) and printing speed ($v$).

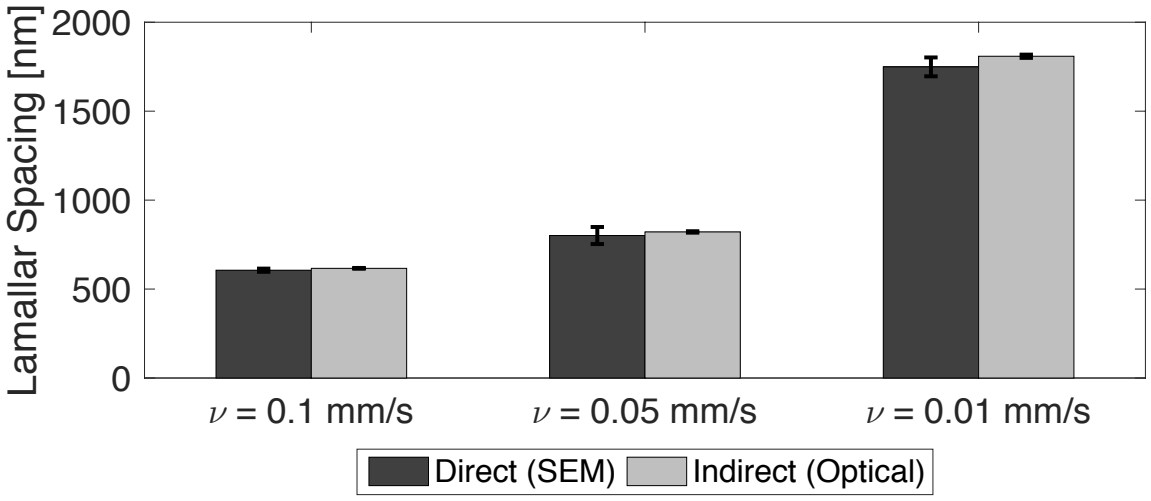


**Figure S4.** Comparison of lamellar spacing measured directly from SEM images to that estimated from the measured first order diffraction response.

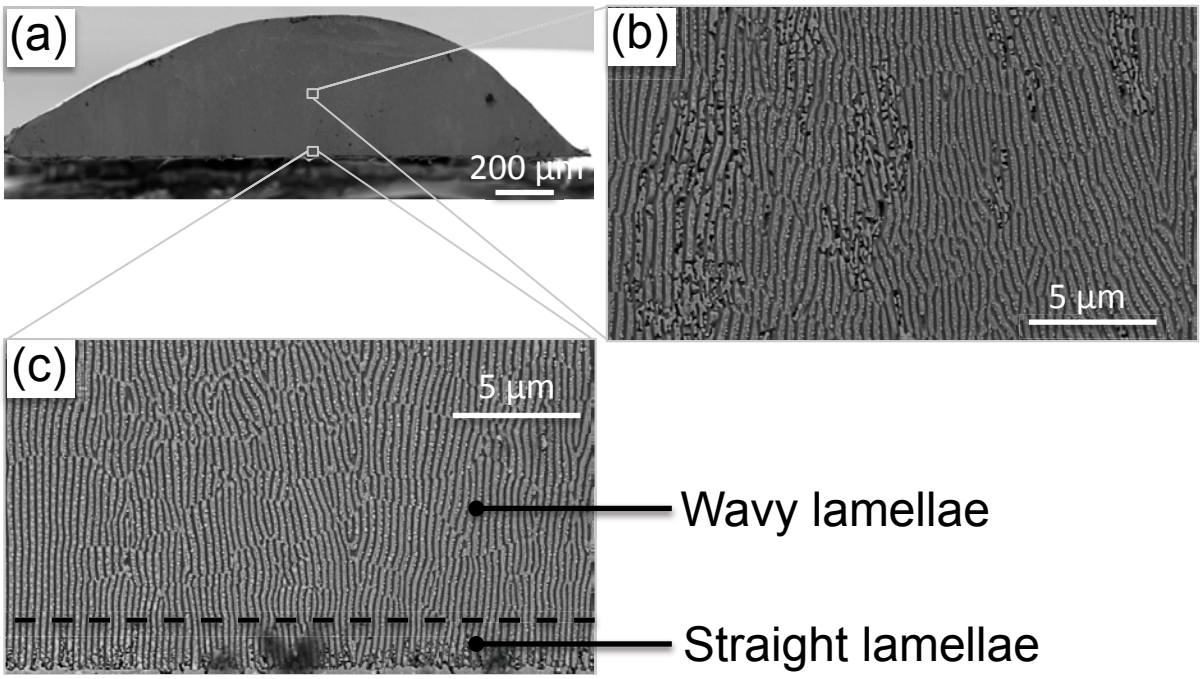


**Figure S5. Representative images of a printed eutectic AgCl-KCl filament.** (a) SEM of the filament cross-section. Higher magnification views of the (b) filament center revealing the presence of wavy lamellae and (c) filament-substrate interface that contains both wavy and straight lamellar regions. Dotted line denotes the boundary between these two regions. This filament was printed using a nozzle diameter = 1 mm, nozzle temperature ~ 400°C, substrate temperature ~ 25°C, and $v = 0.35$ mm·s$^{-1}$.

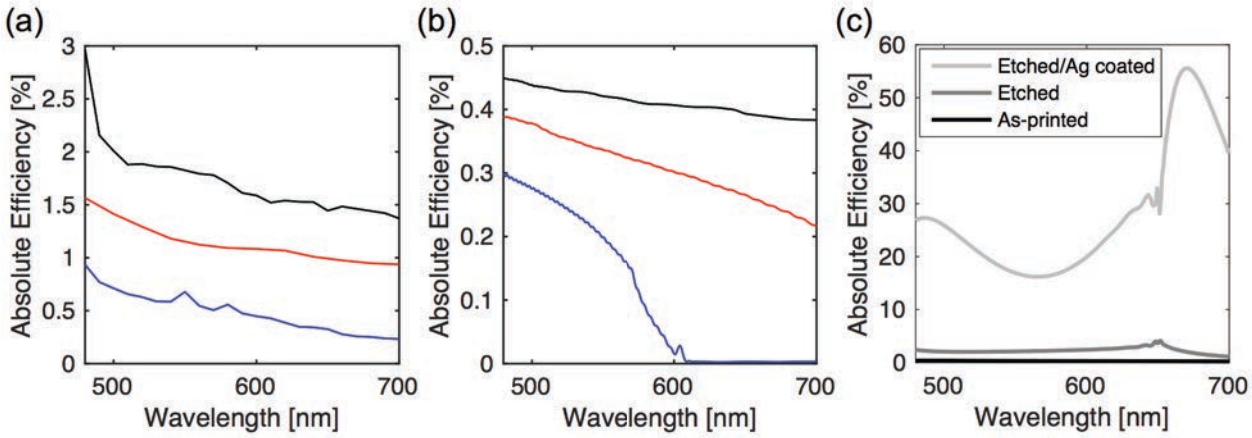


**Figure S6. Absolute diffraction efficiencies.** (a) Measured absolute diffraction efficiency for eutectic filaments printed at $v = 0.01$ mm·s$^{-1}$ ($L \approx 1749$ nm) (black), $v = 0.05$ mm·s$^{-1}$ ($L \approx 801$ nm) (red), and $v = 0.1$ mm·s$^{-1}$ ($L \approx 606$ nm) (blue). (b) Simulated absolute efficiency for eutectic filaments. Colors are matched to corresponding print speeds and lamellar spacings in (a). (c) Simulated absolute diffraction efficiency for as-printed ($v = 0.05$ mm·s$^{-1}$), KCl-etched, and KCl-etched and coated with silver (450 nm thick), where $L \approx 801$ nm.

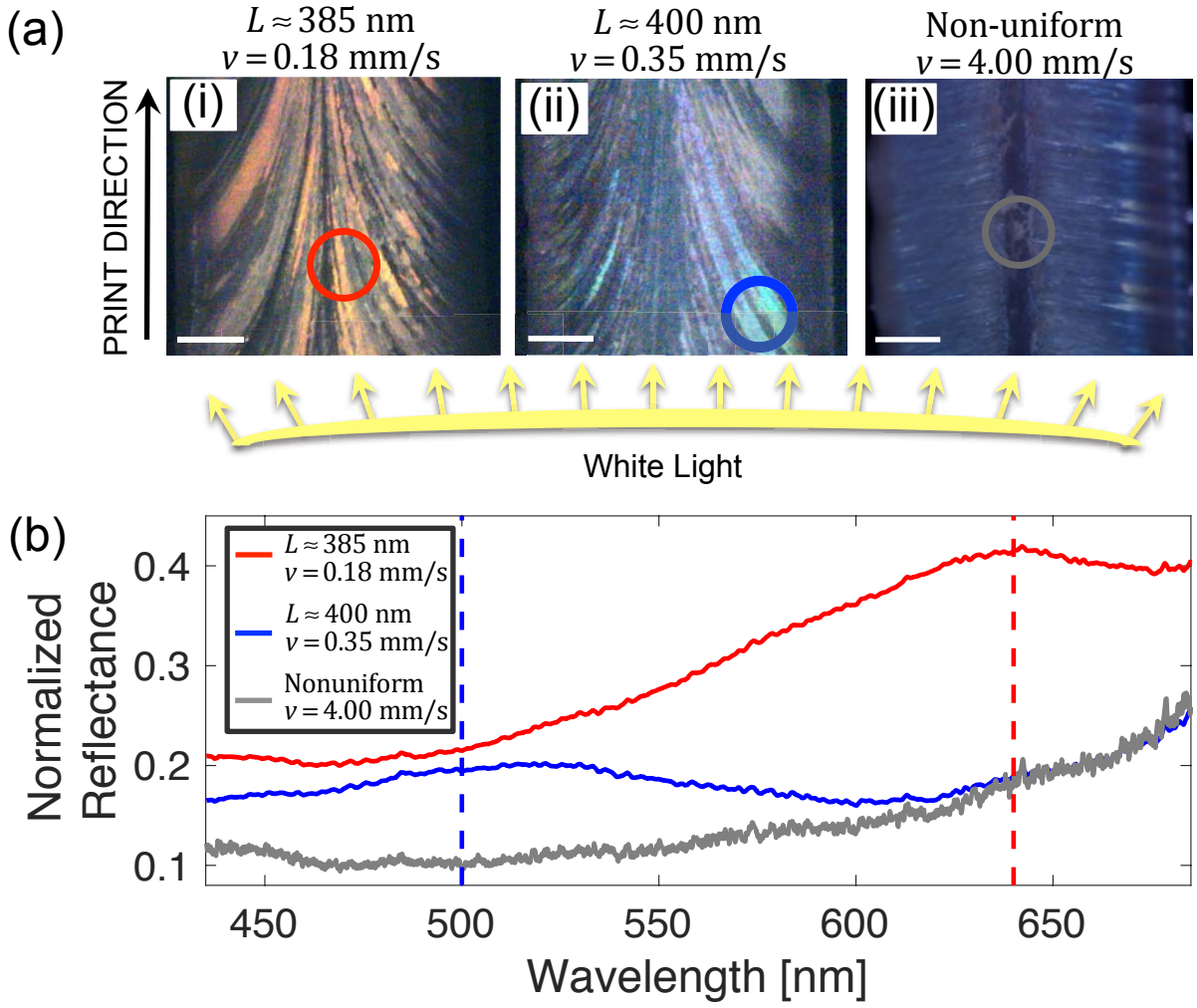


**Figure S7. Printed eutectic AgCl-KCl filaments exhibit structural color.** (a) Optical micrographs of top surface of filament printed at $v = 0.18$ mm·s$^{-1}$ (i), $v = 0.35$ mm·s$^{-1}$ (ii), and (iii) $v = 4.00$ mm·s$^{-1}$. Schematic at bottom shows direction of white light source. Colored circles mark locations from where spectral measurements were obtained. Corresponding lamellar spacings and print speeds are noted above each micrograph. Scale bars are 400 μm in length. (b) Normalized reflectance measurements obtained from locations marked in (a). Observed peaks for samples displaying structural color are marked by vertical dotted lines at corresponding wavelengths, and are color-matched to their respective spectra. [Note: No reflectance peaks are observed in the non-uniform sample.]

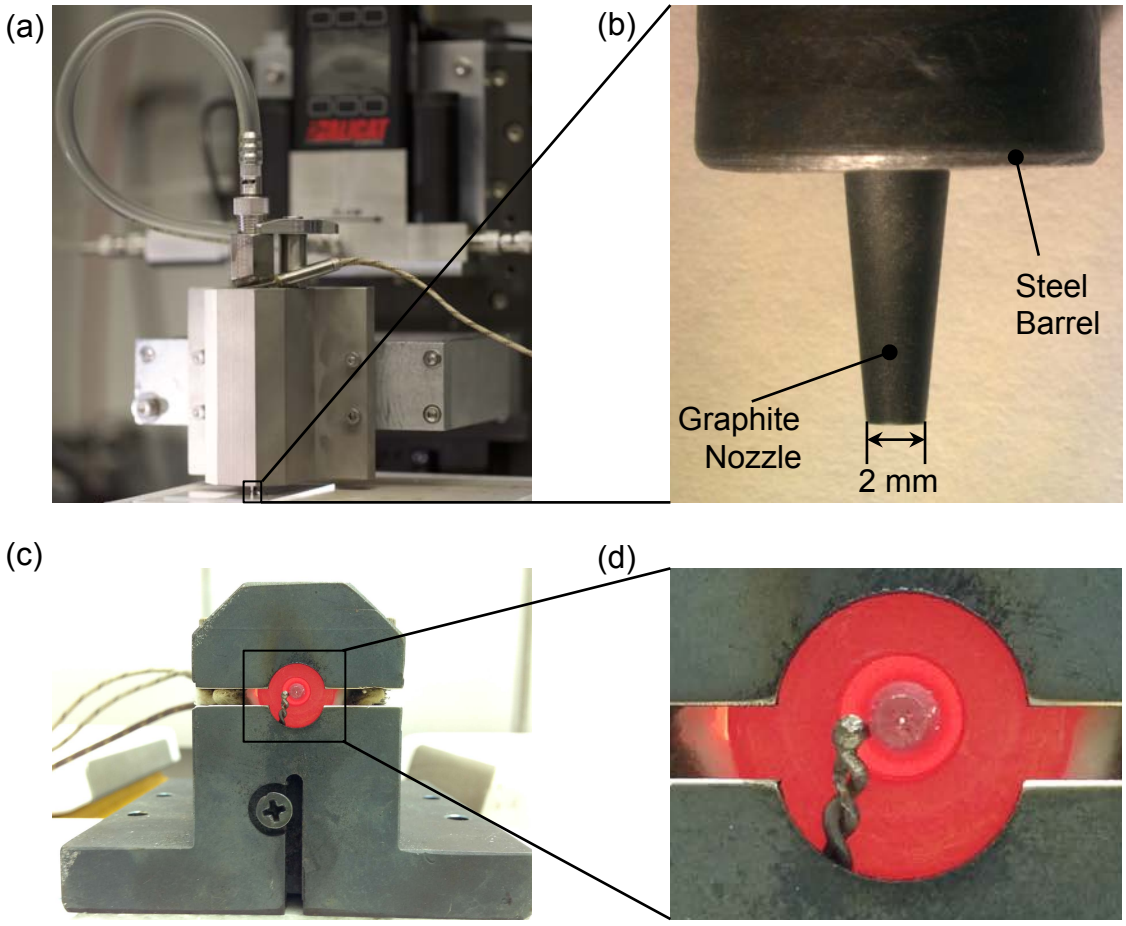


**Figure S8.** (a) Representative image of HOT printhead, (b) High magnification image of nozzle tip, and (c,d ) Bottom view of HOT printhead and high magnification view of the 200 μm nozzle orifice (white color) operating at 700°C, respectively.

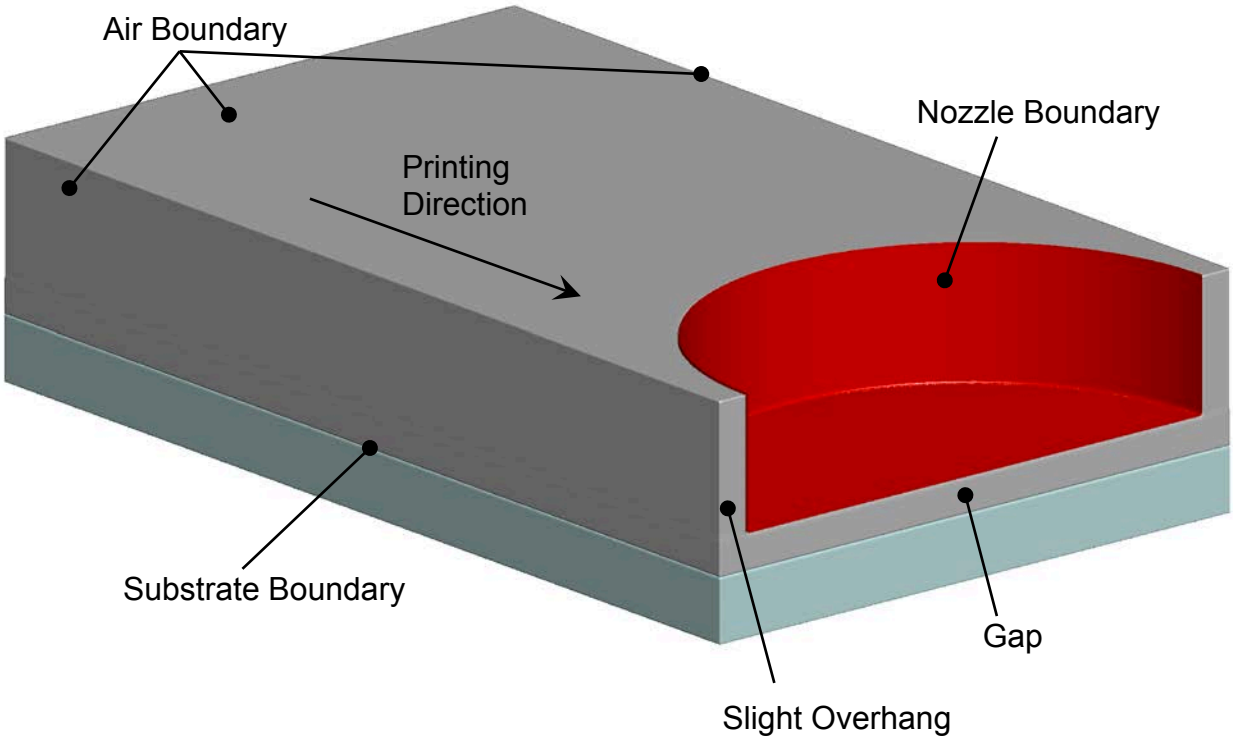


**Figure S9.** Schematic illustration of 3D heat transfer simulation (not drawn to scale) highlighting key boundaries.

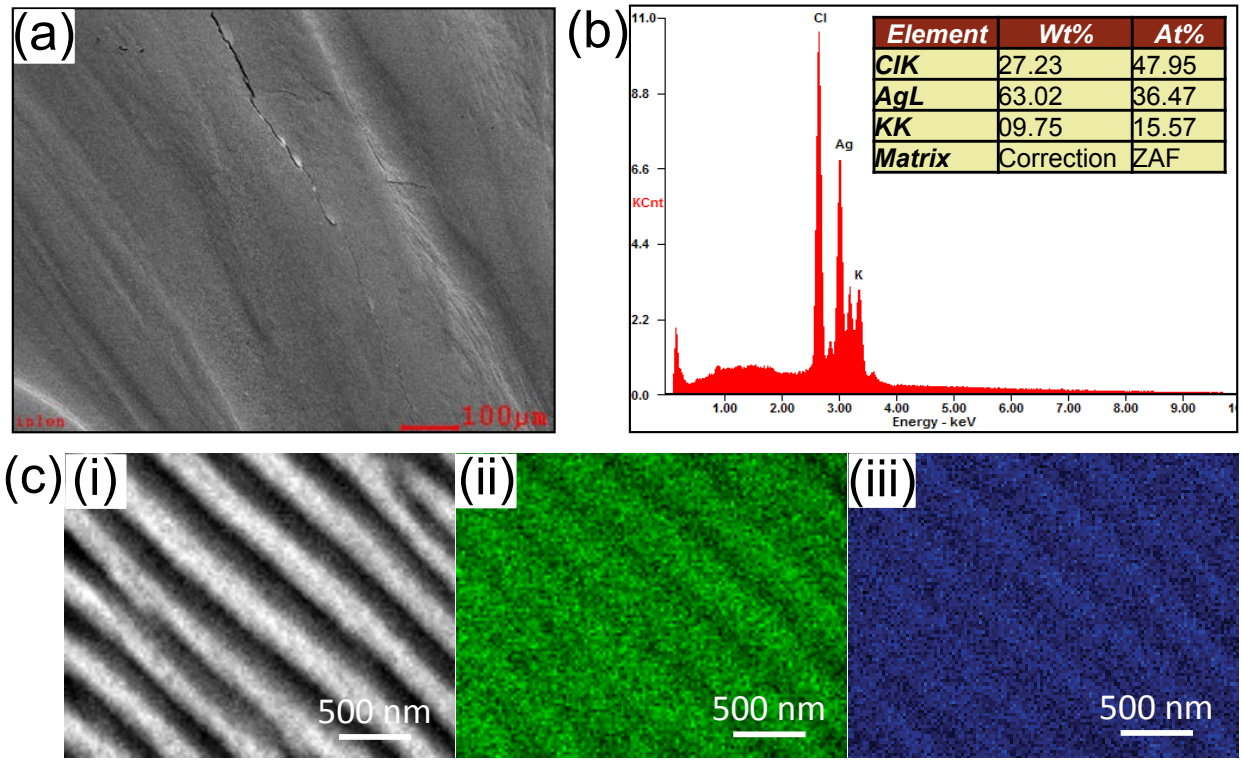


**Figure S10. Composition of printed eutectic AgCl-KCl filaments.** (a) SEM image of top surface of representative printed filament. (b) Corresponding EDS spectra (main) and extracted composition ratio of Cl, Ag, and K (inset). (c) SEM image and (ii-iii) corresponding elemental mapping (EDS analysis) of the lamellar features, where green denotes silver and blue denotes potassium. Representative sample printed at $v = 0.25$ mm·s$^{-1}$.

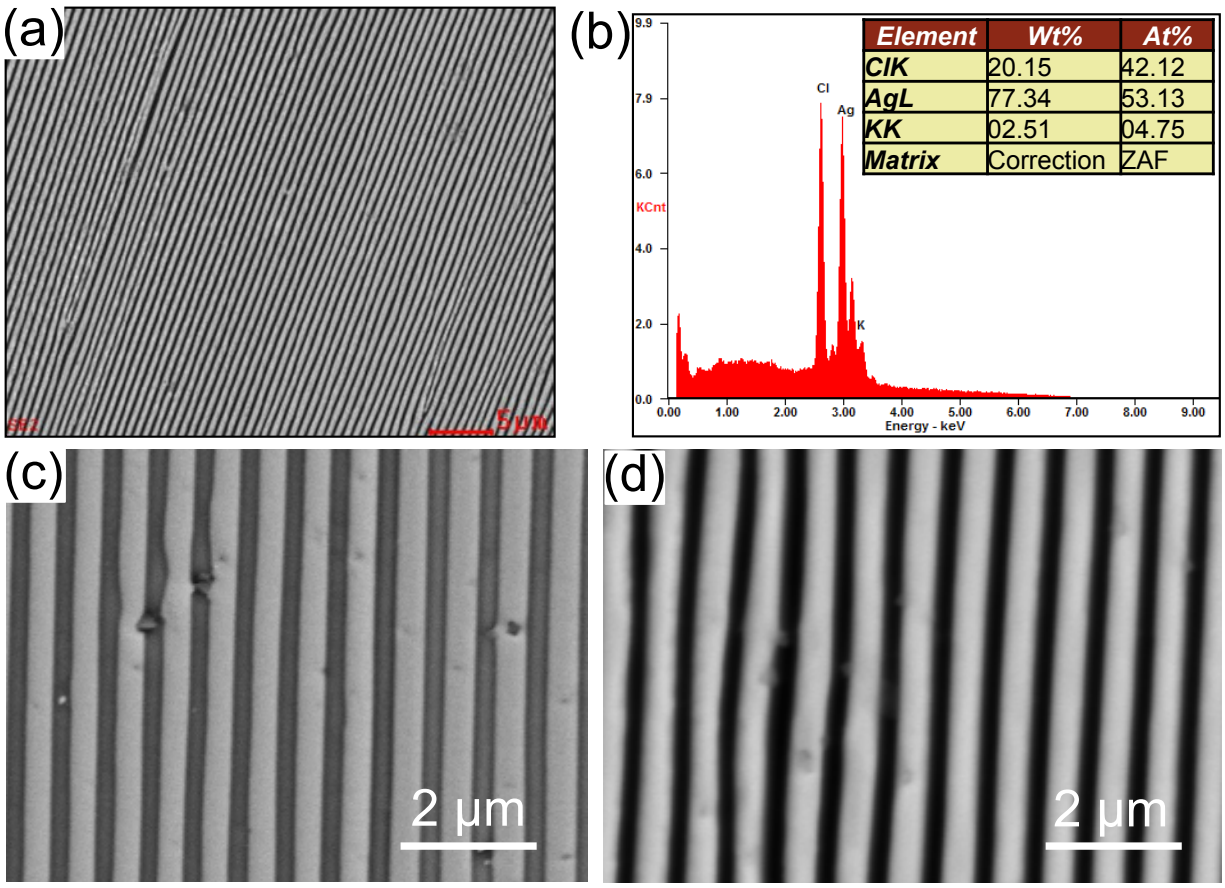


**Figure S11. Etching of printed eutectic AgCl-KCl filaments.** (a) SEM image of bottom of filament. (b) Corresponding EDS spectra (main) and extracted composition ratios of Cl, Ag, and K (table inset). (c) SEM image of bottom of un-etched sample. (d) SEM image bottom of etched sample. Representative sample printed at $v = 0.05$ mm·s$^{-1}$.

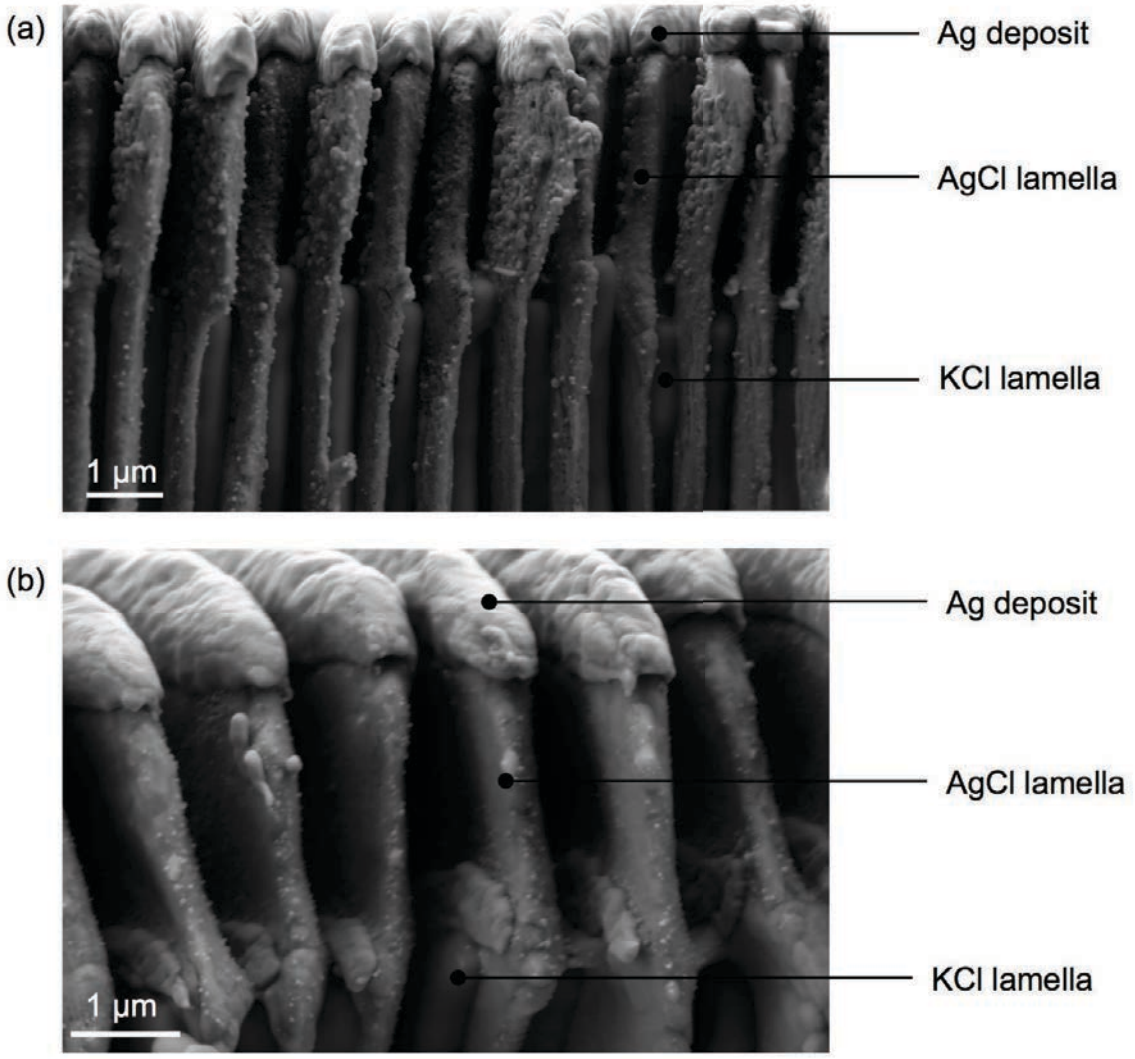


**Figure S12. Cross-sectional view of modified printed eutectic filaments.** (a) SEM image of bottom cross-section of the printed filament after KCl etching and silver coating. (b) Higher magnification SEM image. Representative sample printed at $v = 0.05$ mm·s$^{-1}$.

**Table S1.** Quantities used in parameterizing the phase field simulations.

| Quantity | Symbol | Value | Reference |
|---|---|---|---|
| Thermal diffusivity of solid eutectic | $\alpha_S$ | $1.86\times10^{-6}$ $m^2 \cdot s^{-1}$ | [1, 2] |
| Thermal diffusivity of liquid eutectic | $\alpha_L$ | $2.36\times10^{-7}$ $m^2 \cdot s^{-1}$ | [3] |
| Thermal conductivity of solid eutectic | $k_S$ | 3.25 W $m^{-1} \cdot K^{-1}$ | [1, 2] |
| Thermal conductivity of liquid eutectic | $k_L$ | 0.45 W $m^{-1} \cdot K^{-1}$ | [3] |
| Heat capacity of solid eutectic | $c_S$ | 417 J $kg^{-1} \cdot K^{-1}$ | [1, 2] |
| Heat capacity of liquid eutectic | $c_L$ | 519 J $kg^{-1} \cdot K^{-1}$ | [3] |
| Temperature of air | $T_{\mathrm{air}}$ | 25°C | Experiment |
| Temperature of substrate | $T_{\mathrm{sub}}$ | 25°C | Experiment |
| Temperature of nozzle | $T_{\mathrm{nozzle}}$ | 400°C | Experiment |
| Heat transfer coefficient to air | $h_{\mathrm{air}}$ | 10 W $m^{-2} \cdot K^{-1}$ | [4] |
| Heat transfer coefficient to substrate | $h_{\mathrm{sub}}$ | $2\times10^3$ W $\cdot m^{-2} \cdot K^{-1}$ | Experiment |
| Liquidus slope of AgCl | $m_{AgCl}$ | -542 K·$mol^{-1}$ | [5] |
| Liquidus slope of KCl | $m_{KCl}$ | 837 K·$mol^{-1}$ | [5] |
| Eutectic temperature | $T_E$ | 319°C | [5] |
| Eutectic composition | $C_E$ | 30 mol% | [5] |
| Composition of AgCl at $T_E$ | $C_{AgCl}$ | 0 mol% | [5] |
| Volume fraction of KCl at $T_E$ | $V_E$ | 38 vol.% | Calculated |
| Composition of KCl at $T_E$ | $C_{\mathrm{KCl}}$ | 100 mol% | [5] |

| | | | |
|---|---|---|---|
| AgCl-Liquid interfacial energy | $\sigma_{AgCl-L}$ | 154 mJ·m$^{-2}$ | Assume same as $\sigma_{KCl-L}$ |
| KCl-Liquid interfacial energy | $\sigma_{KCl-L}$ | 154 mJ·m$^{-2}$ | [6] |
| AgCl-KCl interfacial energy | $\sigma_{AgCl-KCl}$ | 154 mJ·m$^{-2}$ | Assume same as $\sigma_{KCl-L}$ |
| Latent heat of fusion per unit mass for eutectic | $L_{\mathrm{E}}$ | $1.4\times10^{5}$ J·kg$^{-1}$ | [7] |
| Latent heat of fusion per unit volume for AgCl | $L_{AgCl}$ | $5.12\times10^{8}$ J·m$^{-3}$ | [7] |
| Latent heat of fusion per unit volume for KCl | $L_{KCl}$ | $6.93\times10^{8}$ J·m$^{-3}$ | [7] |
| Thermal gradient for edge of filament | $G_{edge}$ | $1.5\times10^{7}$ K·m$^{-1}$ | 3D heat transfer simulations |
| Thermal gradient for center of filament | $G_{cent}$ | $9.5\times10^{5}$ K·m$^{-1}$ | 3D heat transfer simulations |
| Diffusion coefficient | $D$ | $3.79\times10^{-9}$ m$^{2}$·s$^{-1}$ | Experiment* |

*To our knowledge, the diffusion coefficient of AgCl-KCl has not been measured at the eutectic composition and temperature. The diffusion coefficient was calculated by fitting the Jackson-Hunt relationship[8] to the experimental results for lamellar spacing versus solidification velocity (**Figure 3d**). Using the other known physical parameters, the diffusion coefficient was estimated. The value of $3.79\times10^{-9}$ m$^{2}$·s$^{-1}$ is within the range of $K^{+}$ diffusivity in liquid AgCl or KCl reported in the literature.[9, 10]

**Table S2.** Properties of eutectic AgCl-KCl ink at HOT nozzle temperature ($T_H = 400°C$) and eutectic temperature ($T_E = 319°C$).

| Quantity | Symbol | Value at $T_H$ | Value at $T_E$ | Reference |
|---|---|---|---|---|
| Density | $\rho$ | 3.7 g $m^{-3}$ | 3.8 g·$m^{-3}$ | Extrapolated from [11] |
| Surface tension | $\sigma$ | 145 mN·$m^{-1}$ | 151 mN·$m^{-1}$ | Extrapolated from [11] |
| Viscosity | $\mu$ | 3.1 mPa·s | 4.7 mPa·s | Extrapolated from [11] |

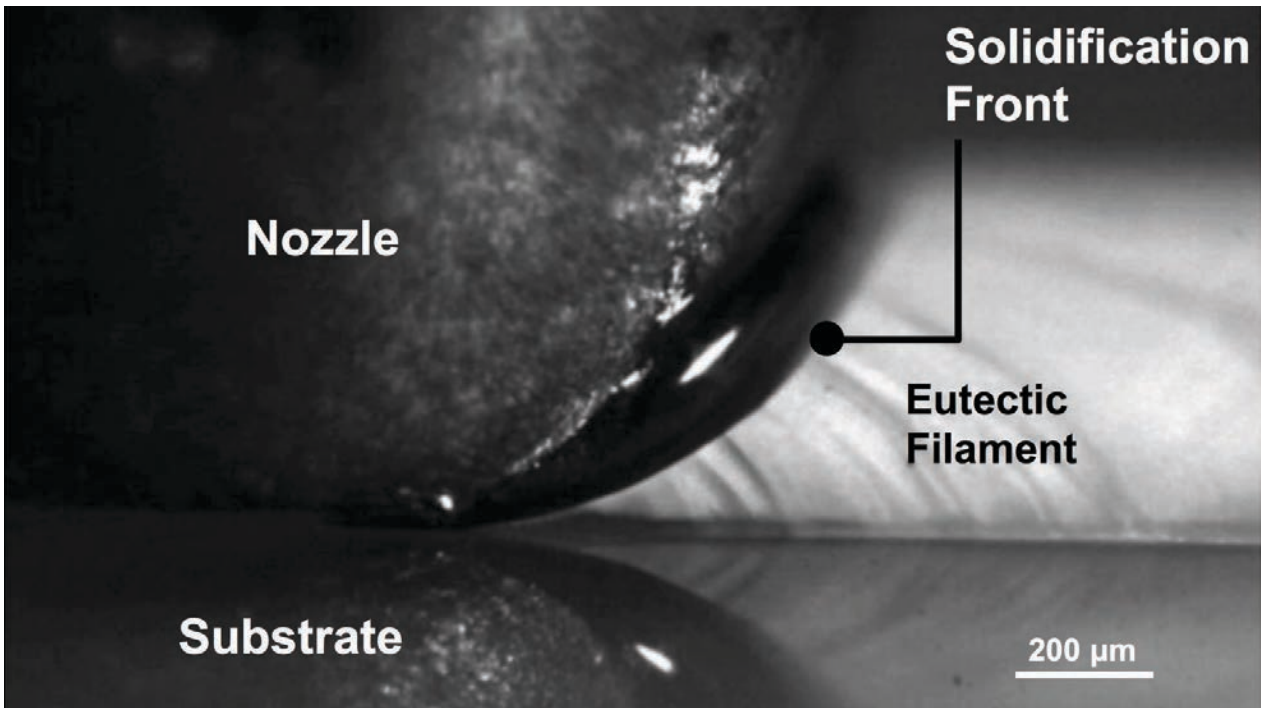


**Movie 1. HOT-DIW of molten AgCl-KCl ink.** Side view of printed eutectic AgCl-KCl filament at $v$ = 0.1 mm·s$^{-1}$.

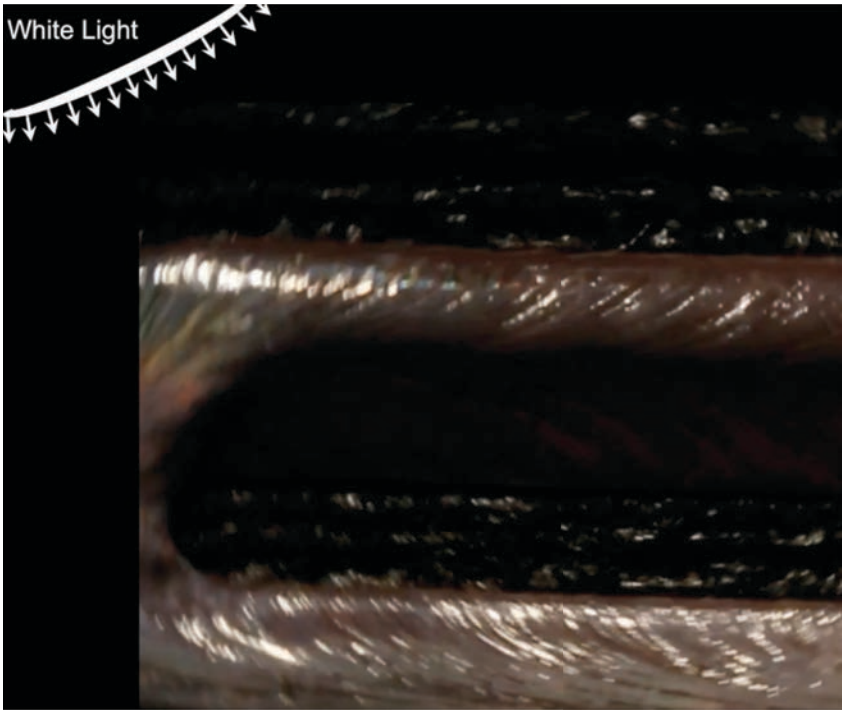


**Movie 2. Structural color observed for printed eutectic filaments.** Top view of printed eutectic filament (2 mm wide, $v$ = 0.18 mm·s$^{-1}$) reveals that their structural color (red) switches on and off depending on orientation of lamellar features with respect to the white light source.

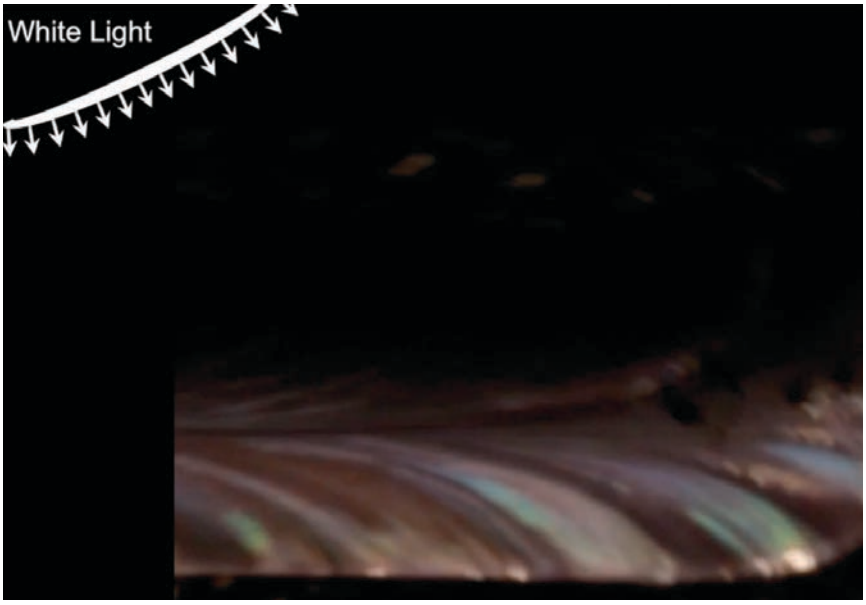


**Movie 3. Structural color observed for printed eutectic filaments.** Top view of printed eutectic filament (2 mm wide, $v$ = 0.35 mm·s$^{-1}$) reveals that their structural color (blue) switches on and off depending on orientation of lamellar features with respect to the white light source.

**References**

[1] CRYSTRAN, http://www.crystran.co.uk/optical-materials/silver-chloride-agcl (accessed June 5 2016).
[2] CRYSTRAN, http://www.crystran.co.uk/optical-materials/potassium-chloride-kcl (accessed June 5 2016).
[3] Y. Nagasaka, N. Nakazawa, A. Nagashima, International Journal of Thermophysics 1992, 13, 555.
[4] J. H. Whitelaw, http://thermopedia.com/content/660/ (accessed June 5 2016).
[5] E. Fischer, Journal of Phase Equilibria 2003, 24, 228.
[6] C. R. P. Rodrigues, M. S. F. Silva Fernandes, The European Physical Journal D 2007, 41, 113.
[7] W. T. Thompson, S. N. Flengas, Canadian Journal of Chemistry 1971, 49, 1550.
[8] J. D. Hunt, K. A. Jackson, Transactions of the Metallurgical Society of AIME 1966, 236, 843.
[9] P. C. R. Rodrigues, F. M. S. Silva Fernandes, Eur. Phys. J. D 2006, 40, 115.
[10] V. S. Znamenskii, P. F. Zil'berman, P. A. Savintsev, E. A. Goncharenko, Inorganic Materials 1996, 32, 536.
[11] G. J. Janz, N. P. Bansal, Journal of Physical and Chemical Reference Data 1975, 4, 871.